

STAR FORMATION IN S0 GALAXIES

Jo Ann Eder
N.A.I.C., Arecibo Observatory
P. O. Box 995
Arecibo, PR 00613
U.S.A.



ABSTRACT

The large range in gas content found for S0 galaxies is difficult to explain. While very low upper limits ($< 10^7 M_{\odot}$) can be placed on the mass of atomic hydrogen of some systems, as many as a fourth of the galaxies classified as S0 in the UGC may have gas surface densities as high as those found for Sa or Sb galaxies. This paper compares the star formation properties of gas-rich S0 and Sa galaxies with gas-poor S0's, in order to determine the importance of a gas surface density threshold for star formation, both globally and locally. All of the gas-rich S0's studied manifest low surface brightness structure, either in blue light or in H_{α} -N II emission line regions, or in both. Comparable images of the gas-poor S0's show no structure except dust lanes, while the intermediate S0's, with marginal gas contents, have diffuse disk line emission associated with very faint blue arms. The local gas surface densities, indicated by maps of the atomic gas for two gas-rich S0's, UGC 2367 and UGC 5419, are consistent with the requirement of a threshold gas density for the appearance of star formation.

1. The S0 Galaxy as a Transition Classification

Hubble originally proposed the S0 classification as a transition between spiral and elliptical galaxies before he actually identified specific galaxies as S0's. Since the prominence of arm structures, as outlined by bright star formation regions, increased along the spiral sequence from Sa to Sd, Hubble reasoned that galaxies must exist with smooth, featureless disks, which lacked arms or obvious star formation regions.

In other morphological classification systems, S0 galaxies are also identified as disk galaxies devoid of any indication of star formation which could be discerned from photographic plate images (Buta, this volume). However, S0 galaxies occupy a large volume of parameter space when other parameters, such as disk-to-bulge ratio (D/B), gas content, and rotational velocity, are considered. These may be the very properties which drive a galaxy's evolution and determine its morphological classification. (Larson, this volume) The distribution of D/B for S0 galaxies is similar to that for Sa - Sb galaxies (Kent 1985, Eder 1990). The rotational velocities of S0 galaxies, like those of Sa's, tend to be higher for a given luminosity than those of later types (Rubin *et al.* 1985, Giovanelli *et al.* 1986). The S0 hybrid neutral hydrogen surface density (σ_{HI} , derived using the *optical* diameter) has a large range, from values typical of Sa and Sb galaxies to upper limits well below that detected within spiral galaxies of similar size. In a recent 21 cm survey of massive early-type disk galaxies, half of the S0 galaxies were detected and half of these detections had values of σ_{HI} as large as that found for Sa galaxies. (Eder, Giovanelli, and Haynes 1991, hereafter EGH).

If the star formation rate depends on gas density (Schmidt 1959, Kennicutt 1989, Larson, this volume), it is surprising that galaxies of similar σ_{HI} have such different levels of star formation such that some would be classified as spirals and others as S0's. Buta cautions that low surface brightness features, such as arms or rings, can be missed on underexposed plates. Could these gas-rich S0 galaxies be either misclassified spirals, or examples of the anemic spirals with low surface brightness structure of van den Bergh's parallel sequence classification system? (van den Bergh 1976)

The remainder of this paper will examine these possibilities and will discuss the relation between σ_{HI} and star formation, both globally and locally. CCD images in B, R, and continuum-subtracted $\text{H}\alpha$ - N II will be compared for four samples: Sa galaxies, gas-rich S0's, gas-poor S0's and marginal S0's, with values of σ_{HI} intermediate between the gas-rich and the gas-poor samples. Also, VLA maps of the atomic gas in two gas-rich S0's will be examined to determine the local H I surface densities near regions of $\text{H}\alpha$ emission.

2. Are Gas-Rich S0's Misclassified?

The galaxies to be imaged were chosen from a 21 cm survey of massive, early-type disk galaxies (EGH), and from a survey of isolated galaxies (Haynes and Giovanelli 1984, hereafter HG), both performed with the Arecibo radio telescope. The galaxies were assigned to the four samples according to their morphological classifications in the UGC (Uppsala General Catalogue of Galaxies, Nilson 1973) and to the value of their hybrid H I surface densities, σ_{HI} , calculated with the integrated H I flux, corrected for pointing errors and source extent, and with diameters measured from the POSS plates, as reported in EGH and HG. The values of σ_{HI} for the four samples are given in Table 1.

The optical images were obtained during two observing sessions: one in March, 1989, at the CTIO 0.9 m telescope and the other in November, 1990, at the KPNO 0.9 m telescope. The CCD cameras were equipped with a TI chip with a scale of 0.49 arcsec per pixel at CTIO, and a TEC chip with a scale of 0.79 arcsec per pixel at KPNO. The images were bias-subtracted and flatfielded utilizing the standard procedures within IRAF. The galaxies were imaged with two 80 Å wide filters, one which included the redshifted $\text{H}\alpha$ and N II lines and the other chosen to measure the continuum near the $\text{H}\alpha$ - N II lines. After sky-subtraction and corrections for extinction and slight differences in the filter response functions, the continuum image was subtracted from the $\text{H}\alpha$ - N II image.

A comparison of the R, B, and continuum-subtracted $\text{H}\alpha$ images provides clues to an explanation for the large range in S0 gas densities. Based only on the R images, the galaxies classified as Sa show definite arm structure while those classified as S0 have apparently smooth disks. However, the B images of the gas-rich S0's reveal faint, low surface

Table 1. $H\alpha$ Morphology of Sa and S0 Galaxies

Sample σ_{HI} in $M_{\odot}pc^{-2}$	UGC	Type UGC, RC2	$H\alpha$ Morphology
Sa: $\sigma_{HI} > 3$	6695	Sa	central, arms
	6746	Sa, SA(r)0/a	central, ring
	9006	S...	arms
	9696	Sa	central, arms
	9960	Sa	central, no arms
Gas Rich S0's: $\sigma_{HI} > 3$	491	S0, Sa(r)0	ring (skewed)
	550	S...	flocculent knots
	2367	S0	central, arms
	2774	S0	central, ring
	3201	SB0/SBa, (r)SB(s)0/a	central, open arms, knots
	5419	S0	central, ring, arms
	6322	S0, SA0+ or 0/a	none
	7198	SB0	central, short arms
	8343	S...	central, faint disk
	12760	S0?	inner ring
12840	SB0, (R)SAB(s)0	central, pseudo-ring, arms	
Marginal S0's: $\sigma_{HI} = 1.5-3$	818	SB0	faint ring (skewed)
	2357	S0, SA0	very little - diffuse disk
	4345	S0a	very little
	5159	Sa?	central, diffuse ring
	5239	S0	faint arms, diffuse disk
	5966	S0a	central
Gas Poor S0's: $\sigma_{HI} < 1.5$	4312	S0/Sa	central
	4875	S0a	central

brightness structure, sometimes including the blue knots associated with active star formation regions. The H_{α} images indicate star formation activity, concentrated in tight arcs or rings, along many of these low surface brightness features. Details of the H_{α} morphology for the program galaxies are given in Table 1 along with the classifications from the UGC and the RC3 (deVaucouleurs *et al.* 1991). Qualitatively, the gas-rich S0's have as much star formation activity as is seen in the Sa galaxies, although it is frequently concentrated in very sharply defined regions. The S0's with marginal gas content show only faint, diffuse H_{α} emission, if any. The gas-poor S0's have only central emission.

All four samples contain galaxies with central emission. Long-slit spectra of UGC 4312, UGC 5966, UGC 6695, and UGC 6746 show that most of the central emission is due to the N II λ 6584 line. This is likely to be the case for the other galaxies with central emission, as well. Most of the nuclear emission detected in early-type disk galaxies has N[II] λ 6584/ H_{α} ratios greater than one and therefore emanates from low-ionization regions of gas. (Keel 1983 and Phillips *et al.* 1986)

The H_{α} images of the Sa galaxy UGC 9960 and the S0 UGC 6322 are puzzling. Faint, smooth arms are clearly present on the blue images but not on the H_{α} images. These two galaxies could be examples of transition objects, caught between the last epoch of star formation and the fading of the blue stars it produced. If a threshold gas density is necessary for star formation (Kennicutt 1989), the gas within the Sa's and gas-rich S0's may be close to this threshold value globally. In local regions, where the gas density is enhanced, the σ_{HII} may rise above the threshold value so that star formation can occur.

Besides the expected density enhancement due to spiral waves, several low-order resonances may be responsible for much of the H_{α} morphology observed in our samples. The nuclear ring of H_{α} emission seen in UGC 12760 may be a manifestation of star formation triggered by an abrupt perturbation of stable orbits at the Inner Lindblad Resonance, as discussed for NGC 4321 by Arsenault *et al.* (1988). Knots of star formation are clearly present as distinct beads at both ends of the bar in UGC 3201. Kenney and Lord (1991) observed large CO complexes associated with the bright H II regions located at the bar-spiral arm transition zone in M83 and found the kinematics of the gas to be consistent

with a gas density enhancement due to orbit crowding at the intersections of the bar and the spiral arms. The prevalence of H_{α} rings and pseudo-rings in the gas-rich samples could be associated with the Outer Lindblad Resonance (Schwarz 1981 and Buta and Crocker 1991).

3. Threshold Gas Surface Density

In order to determine the connection between the gas content and the star formation in these anemic galaxies, we have mapped the neutral hydrogen for two of the gas-rich S0 galaxies, UGC 2367 and UGC 5419 (Eder & Haynes 1993). The observations were made in December, 1990, with the VLA in the C array with a velocity resolution of 21 km s^{-1} and a beam width at FWHM of $18'' \times 18''$ for UGC 2367, and of 10 km s^{-1} and $24'' \times 20''$ for UGC 5419. Cleaned, continuum-subtracted maps of the total H I surface density and the velocity field for each galaxy were made using programs in AIPS.

The channel maps are typical for rotating gas disks. All of the blue light of the galaxies falls within regions in which the atomic gas surface density, corrected for inclination, is greater than $1 M_{\odot} \text{pc}^{-2}$. For UGC 5419, there are patches of H I within the star formation regions with surface densities of $2.4 M_{\odot} \text{pc}^{-2}$. The map of the total H I content of UGC 2367 is shown in Figure 1. The blue extent of the optical image is given by the outer dashed-line ellipse and the extent of the H_{α} emission is indicated by the inner ellipse. The gaseous disk extends well beyond the optical image, but the surface densities in the outer regions are less than $1 M_{\odot} \text{pc}^{-2}$. The location of the arcs of H_{α} emission are shown by the letters a, b, c, d, and e.

A rotation curve was derived for UGC 2367 since it is highly inclined ($\epsilon = 0.72$). The critical gas surface density necessary for the instability of a gaseous disk was calculated using the formula of Kennicutt (1989) for a gas disk with a flat rotation curve, with a constant velocity dispersion of 6 km s^{-1} , and with a stability parameter of 0.67, as estimated for Sc galaxies. The total gas surface density for the regions of star formation was estimated from the H I maps, assuming a mean ratio of molecular to neutral hydrogen gas of 1.4, as found for S0's by Lees *et al.* (1991). In Table 2, the values of the critical gas density are compared

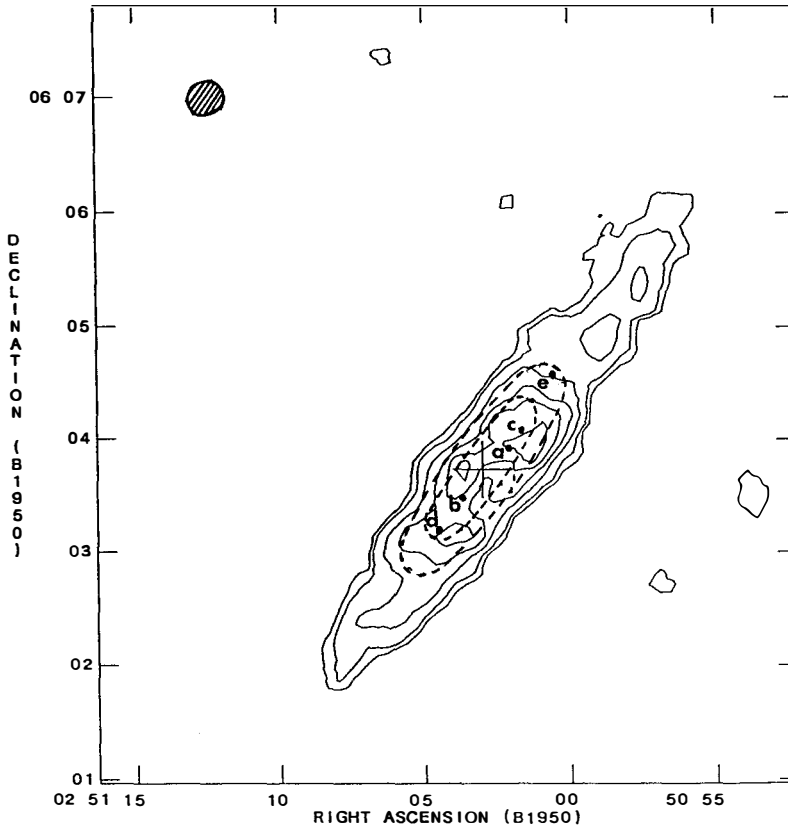


Figure 1. Contour plot of the zeroth moment map for UGC 2367 which shows the atomic gas distribution. The extent of the star formation is indicated by the inner dashed ellipse and that of the optical image (r_{25}) by the outer dashed ellipse. The contours indicate gas surface densities of 0.5, 1, 2, 3, 4, and 5 $M_{\odot} \text{pc}^{-2}$. The locations of the sharp arcs of star formation from the H_{α} image are shown by the letters a, b, c, d, and e. The beam is shown by the hatched area in the upper left.

Table 2. Gas Densities in Regions of Star Formation for UGC 2367

	r kpc	σ_{thresh} $M_{\odot} \text{pc}^{-2}$	σ_{gas} $M_{\odot} \text{pc}^{-2}$
a	5.4	7.3	11.8
b	5.4	7.3	9.6
c	9.0	7.0	11.8
d	14.4	6.0	9.4
e	22.0	4.7	4.8

with the estimated gas density within the regions of star formation. Within all of the designated star formation regions, the estimated gas density is greater than the critical density.

4. Conclusions

The gas content of S0 galaxies exhibits a large range of values, from amounts comparable to that found in early-type spirals to very low upper limits. Gas-rich S0 galaxies, chosen to have hybrid atomic gas surface densities, σ_{HI} , as large as those commonly found in Sa galaxies ($> 3 M_{\odot}\text{pc}^{-2}$), could all be classified as anemic spirals, with low surface brightness arms and/or distinct regions of star formation. A sample of S0's with marginal gas contents showed less structure and only patchy or diffuse emission on $\text{H}\alpha$ images. Gas-poor S0's had only central line emission. Our $\text{H}\alpha$ images of S0 galaxies show that star formation occurs when $\sigma_{\text{HI}} > 1.5 M_{\odot}\text{pc}^{-2}$ globally, or when local enhancements of the gas density raise the value above a critical value for instability. The hybrid σ_{HI} is thus an important parameter to distinguish between anemic or misclassified spirals and "true" S0's with smooth, featureless disks and no recent star formation.

It is a pleasure to thank Martha Haynes, my collaborator on the VLA observations, and Daniel Puche of NRAO for their help with the intricacies of the VLA and AIPS.

References

- Arsenault, R., Boulesteix, J., Georgelin, Y. & Roy, J. -R. 1988, *A&A*, **200**, 29
 Buta, R. & Crocker, D. A. 1991, *AJ*, **102**, 1715
 de Vaucouleurs, G. et al. 1991, *Third Reference Catalogue of Bright Galaxies* (Springer, Berlin (RC3))
 Eder, J. 1990, Ph. D. thesis, Yale University
 Eder, J., Giovanelli, R. & Haynes, M. P. 1991, *AJ*, **102**, 572 (EGH)
 Eder, J. & Haynes, M. P. 1993, in preparation.
 Giovanelli, R., Haynes, M. P., Rubin, V. C., & Ford, W. K. 1986, *ApJ*, **301**, L7
 Haynes, M. P. & Giovanelli, R. 1984, *AJ*, **89**, 758 (HG)
 Keel, W. C. 1983, *ApJS*, **52**, 227
 Kenney, J. D. P. & Lord, S. D. 1991, *ApJ*, **381**, 118
 Kennicutt, R. C. 1989, *ApJ*, **344**, 685
 Kent, S. M. 1985, *ApJS*, **59**, 115
 Lees, J. F., Knapp, G. R., Rupen, M. P. & Phillips, T. G. 1991, *ApJ*, **379**, 177
 Nilson, P. 1973, *Uppsala General Catalogue of Galaxies*, Uppsala Astron. Obs. Ann., **6**

- Phillips, M.M., Jenkins, C.R., Dopita, M.A., Sadler, E.M. & Binette, L. 1986, *AJ*, **91**, 1062
Rubin, V. C., Burstein, D., Ford, W. K., & Thonnard, N. 1985, *ApJ*, **289**, 81
Schmidt, M. 1959, *ApJ*, **129**, 243
Schwarz, M. P. 1981 *ApJ*, **247**, 77
van den Bergh, S. 1976, *ApJ*, **206**, 883